# Accurate Gait Phase Detection using Surface Electromyographic Signals and Support Vector Machines

Alexander Boschmann, Paul Kaufmann, Marco Platzner

University of Paderborn, Germany

{alexander.boschmann, paul.kaufmann, platzner}@upb.de

***Abstract*—Modern components and materials allow creating increasingly complex, multi-functional prostheses with user-specific intelligent behavior. Complex behavior control, though, has to employ more accurate and precise models of the amputee and his prosthesis to be able to make use of the prosthesis' complete functionality.**

**In this work, we concentrate on the accurate phase detection within a fine-grained and state-full gait model for the continuous level gait. To this, we rely on four electromyography (EMG) sensors, placed at the thigh, and two force sensing resistors (FSR), placed below the heel and the toe. FSRs and a timed gait model are used to automatize EMG data recordings. Afterwards, gait model performance is verified using only EMG data. Here, we use support vector machines to detect muscular activity changes, indicating a new gait phase and therefore, a state switch within the gait model.**

**We show that our approach generalizes well, even when using only 20 to 30 seconds for training. The gait model reaches accuracies of roughly 67% for an amputee and of 75% for a non-amputee individual when using a precise, seven phase level gait model.**

## I. Introduction

Walking is the main form of human locomotion and at the same time the most complex motion sequence. It is accomplished by well-coordinated effort of brain, nerves and 28 major muscles that are needed to control the trunk, joints and limbs, generate the forces to counter gravity and move the body forward with the least possible amount of energy possible [1]. Losing a lower limb has a massive impact not only on mobility but also on many other aspects of amputee's life. By replacing the missing limb with an artificial one, lower limb prostheses are able to immensely improve the amputee's mobility and restore a great amount of quality of life.

Current lower limb prostheses can be divided into three groups: mechanically passive devices, microprocessor-controlled passive devices and powered active devices [2]. Most of the currently commercially available lower limb prostheses are mechanically passive and rely on hydraulic and pneumatic valves and dampers, providing a constant damping moment to the knee joint resulting in a unintuitive control.

In both passive and active microprocessor-controlled lower limb prostheses, sensors in combination with a microprocessor are used to control the damping of the knee joint and help overcome the drawbacks of mechanically passive devices. Microprocessor-controlled prostheses with dynamic knee joint damping reduce energy consumption and allow for various locomotion modes like descending stairs [3]. Some locomotion functions like ascending stairs or walking backwards require considerably more energy at the knee joint and can be currently only executed smoothly with active powered prostheses [4], [5].

By far the most frequently used locomotion mode is level walking. Studies show that compared to non-amputee individuals, above-knee amputees have up to a 60% higher energy consumption [6] and utilize three times the power and torque in the hip [7]. This can result in secondary disorders. In current lower limb prostheses, the amputee has to change the locomotion mode manually, either by a certain prosthesis movement or by muscles co-contraction. Both is often inconvenient and inefficient [8]. Consequently, there is a need for intuitive neural control in order to achieve a smooth and energy efficient gait.

Surface electromyographic (EMG) signals are taken from the skin above relevant muscle groups offer an opportunity to detect an ongoing motion even before the limb starts to change its position in space. Therefore, EMG signals enable the prostheses control to react more quickly compared to systems activated directly by a limb movement. Intuitive control however, needs a more intelligent signal processing as muscle's electric activity and its derivatives mirror only a subset of the provided signal information. Here, pattern matching algorithms help to extract muscle's state on a more detailed level. For a lower-limb prosthesis this might have multiple consequences. Locomotion changes, particularly in situations with a high probability for a change, are detectable with a low latency allowing for a fluent switch in the prostheses behavior. Temporal abnormalities to the regular gait model can be instantly detected allowing for a more robust and adaptive control. Additionally, fine-grained gait partitioning into multiple phases enables the prostheses control to closely monitor whether the amputee is performing a regular movement, or being in a situation of a potential danger. In the latter case, the control might initiate some standard procedures known to the amputee as, e.g., locking of prosthesis active elements, allowing to stabilize the situation in a predictable way.

This paper is structured as follows. Section II reviews related work. In Section III, the gait model used in this work is introduced. In Section IV of this paper, we present an approach for classifying surface EMG signals taken

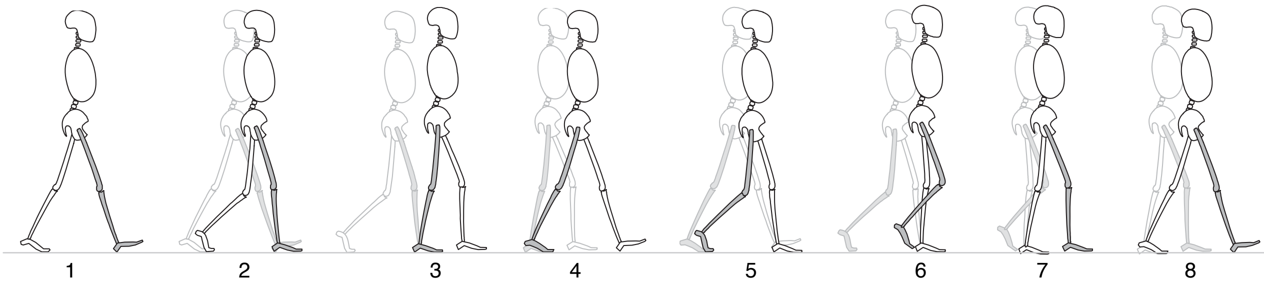


Fig. 1. Gait phases: 1) initial contact 2) loading response 3) mid stance 4) terminal stance 5) pre-swing 6) initial swing 7) mid swing 8) terminal swing

from lower limb muscles using Support Vector Machines. This classifier technique is customized to the amputee and allows us to recognize seven different gait phases with high accuracy. The corresponding experiments are described in Section V. Finally, Section VI concludes the paper.

## II. Related Work

Early attempts to outline the concept of a microprocessor-controlled prosthesis can be found in [9]. Here, the control algorithm divides the gait cycle into phases of equal length while each phase is characterized by an appropriate damping level. The phase detection is performed based on kinematic inputs picked up from both legs.

Hudgins et al. [10] introduced a novel approach to the control of a multifunctional prosthesis. The approach is based on classification of EMG patterns taken from upper limb muscles using artificial neural networks. After a training phase the system is capable of distinguishing discrete movements. Despite its robustness, rapidly changing movements are challenging to the system.

Pappas et al. presented a system based on insole-embedded pressure sensors for gait event detection as heel strike and toe-off [11]. This concept is often applied in current gait analysis systems. We use insole-embedded pressure sensors as a synchronization input during data recordings.

An experimental system capable of predicting four gait phases by using pattern recognition on EMG signals is presented by Hargrove [2] and Huang [12].

Besides EMG and pressure sensors, acceleration sensors and gyroscopes gained popularity for gait analysis in recent work [13], [14], [15].

## III. The Gait Model

In our work we rely on the fine-granular gait model as formalized by Allen et al. [16]. A gait cycle is defined as the time period between two consecutive heel strikes of the same foot. Furthermore, the gait cycle is subdivided into eight gait phases that are indicated in Fig. 1. The gait cycle begins with the *initial contact* when the foot first touches the floor. It is followed by the *loading response*, where the weight bearing lasts on the same foot and continues until the opposite foot is lifted for a swing. Since initial contact is just an event without duration, we combine it with loading response to a phase *initial contact/loading response*. The next phase, *mid stance* initializes single-limb support, when the opposite foot is lifted until the weight is above the forefoot. During *terminal stance*, the heel rises and the opposite foot strikes the ground. This phase is followed by the *pre-swing*, when initial contact of the opposite extremity begins and the toe-off ends, preparing the foot to start the swing. The *initial swing* starts when the foot lifts off from the ground and lasts until it is opposite the stance foot. During *mid-swing*, the foot continues to swing until it is anterior to the tibia of the opposite foot. The *terminal swing* lasts from the end of the mid-swing until the heel strikes the floor, which concludes the gait cycle.

## IV. Sensor System and Feature Extraction

For EMG data acquisition, we use a National Instruments NI USB-6009 analog digital converter [17] to continuously monitor four EMG sensor channels with 13 bit resolution at a sampling rate of 1000 Hz in combination with pre-amplified Biovision EMG sensors [18]. As electrodes we use standard ARBO Ag/AgCl ECG electrodes.

We have placed the four electrode pairs on the following lower limb muscles: M. rectus femoris, M. vastus medialis, M. vastus lateralis and M. biceps femoris. Additionally, a reference electrode was placed on the hip. The electrode placement scheme is presented in Fig. 4. The exact electrode positions are determined specifically for the test subject to obtain pronounced and reproducible signals.

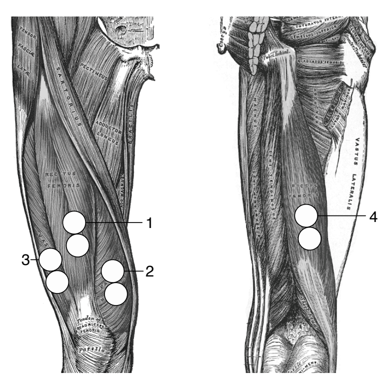


Fig. 4. EMG sensor placement: 1) M. rectus femoris, 2) M. vastus medialis, 3) M. vastus lateralis, 4) M. biceps femoris

In addition to the EMG sensors, we use two custom-designed insole-embedded force sensing resistors (FSR) to analyze pressure underneath the foot. The sensors are situated

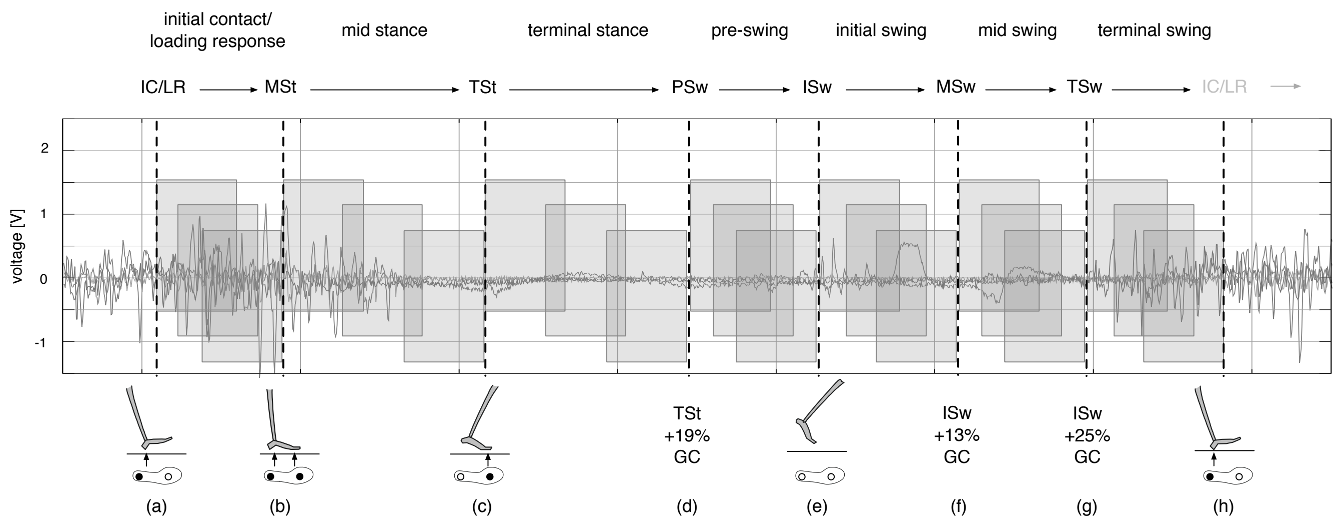


Fig. 2. Division of a gait cycle into gait phases: the beginnings of initial contact/loading response (a), mid stance (b), terminal stance (c) and initial swing (e) can be deduced from pressure sensor data, while the beginnings of pre-swing (d), mid swing (f) and terminal swing (g) are calculated using offsets. The boxes represent 100 ms areas used to compute a single feature.

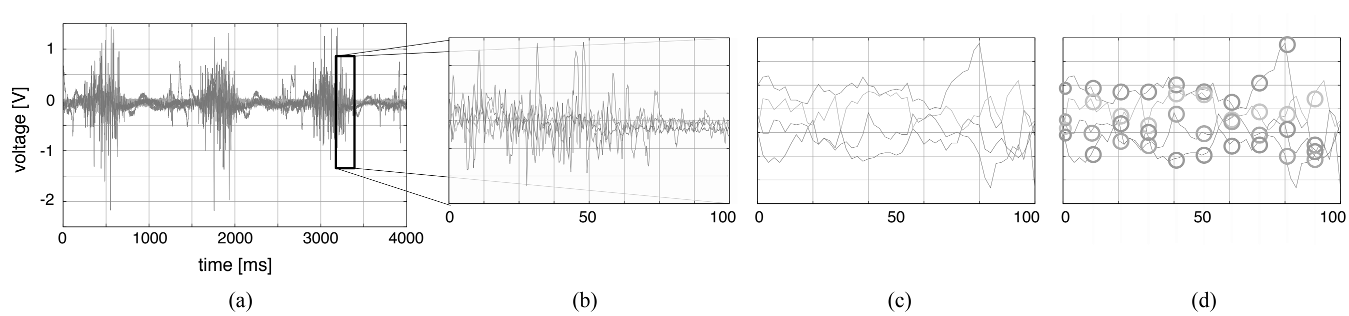


Fig. 3. EMG signal preprocessing: Raw signals for four channels (a). (b) presents 100 ms area corresponding to a box in Fig. 2, and (c) the RMS smoothed signals with the extracted features (d).

under the heel and the toes, enabling the detection of heel strike and toe-off.

Prior to feature extraction, the raw EMG data has to be partitioned into gait cycles which for their part need to be subdivided into individual gait phases. For this purpose, we utilize the pressure sensor data. The schema is illustrated in Fig. 2. The beginning and end of a gait cycle are determined by heel strikes (Fig. 2(a) and (h)). The beginnings of mid stance, terminal stance and initial swing can be defined by corresponding events of the pressure sensor (Fig. 2(b), (c) and (e)). To specify the starting points for pre-swing, mid swing and terminal swing, we rely on gait cycle lengths, given by [1] (Fig. 2(d), (f) and (g)).

Signal processing and feature extraction is done in the digital domain. Based on the raw EMG signals $d_{jkp}$, where $j$ denotes the time index, $k$ the channel ($k = 1 \dots 4$), and $p$ the gait phase ($p = 1 \dots 7$), we extract features in two steps following the approach presented in [19]. First, the steady state signal starting one second after the beginning of a movement is smoothed by a root mean square (RMS) method with a window size of $w_s = 10$ samples. This is shown in Fig. 3(c). The first 100 ms (100 samples at 1000 Hz) of the rectified and smoothed signal are thus given by:

$$d'_{jkp} = [\frac{1}{w_s} \sum_{i=j}^{j+w_s-1} d_{ikp}^2]^{\frac{1}{2}},$$

with $j = 1 \dots 100$. Then, a logarithm-transformed moving average with window size of $w_f = 20$ samples and shift amount of $s_f = 10$ samples is computed from $d'_{jkp}$. A feature then comprises 10 values and is defined as:

$$f_{l_m kp} = -log(\frac{1}{w_f} \sum_{j=l_m}^{l_m+w_f-1} d'_{jkp}),$$

with $l_m = 1 + (m-1) \cdot s_f$, and $m = 1 \dots 10$. Taking all four channels into account, the feature vector for a single movement consists of 40 values which are fed into the classifier. These 40 values are depicted in Fig. 3(d). The feature vectors for all 7 gait phases together form one data set.

## V. Classifiers, Experiments, and Results

In this section we report on the employed pattern matching algorithms, the experiment setup, and the results.

### A. Pattern Matching Algorithms

For EMG signal classification we rely on support vector machines (SVMs) [20], [21]. The key advantage of SVMs is the principle of structural risk minimization which typically yields very good generalization performance compared to other classifier paradigms. In our experiments we employ an exhaustive search on SVM's parameters to identify good performing values for $C$ and $\gamma$. An extensive comparison of SVMs to other classifiers for EMG signal classification can be found in [19].

### B. Experiments

All experiments are executed by an lower-limb male amputee and an male non-amputee subject. Each individual performed three experiments, while repeating each experiment three times. An experiment is defined by the number of gait cycles per minute. In the first two experiments, individuals performed level gait with 40 and 50 cycles per minute. These values were taken from [1] as realistic gait frequency values used by lower limb amputees. A metronome indicated the correct frequencies during the experiments. In the third experiment the test person could chose any desired gait frequency, including variable frequencies. Each experiment repetition was recorded over 60 seconds.

The EMG data was separated into training and test data as follows: we use the first 10 gait cycles of an experiment repetition to train the SVMs. Afterwards, the successive gait cycles within the same experiment repetition are classified by the SVMs.

### C. Results

Tab. I presents the results, partitioned by the performing individual and the gait frequency. As visualized in Fig. 2, data of each gait phase is used to extract three feature sets. With seven gait phases in a single gait cycle, 21 feature sets define a complete gait cycle. Thus, as 10 gait cycles of each of the three experiment repetitions were used for training, a single number in the training accuracy column is averaged over $10 \times 3 \times 21$ feature sets. Similarly, numbers in the training columns are averaged over multiples of $3 \times 21$ feature sets.

| | 40 cyc./min. | | 50 cyc./min. | | var. cyc./min. | |
|---|---|---|---|---|---|---|
| | trn. | tst. | trn. | tst. | trn. | tst. |
| amp. | 76.87% | 67.23% | 79.14% | 68.66% | 74.23% | 64.93% |
| reg. | 85.42% | 75.78% | 86.34% | 75.09% | 84.86% | 73.46% |

TABLE I

RESULTS: TRAINING AND TEST ACCURACY RATES FOR AN AMPUTEE AND NON-AMPUTEE (REG.) LEVEL GAIT WITH 40, 50 AND VARIABLE GAIT FREQUENCY, AVERAGED OVER THREE EXPERIMENT RUNS.

The first conclusion we can draw from Tab. I is, that the non-amputee performs better than the amputee by 7% to 10% during the training and 7% to 9% during the testing. While the test accuracies drops roughly 9% to 11% compared to the training accuracies for both individuals, the non-amputee seems to have the more constant test rates.

## VI. Conclusion

In this paper, we have presented a fine-grained gait model driven by EMG sensors. To verify its performance, we have created an automatic mechanism, synchronizing and partitioning the recorded EMG data by the means of insole-embedded force sensors and a commonly accepted time model of human level gait. While in controlled laboratory conditions the gait time model and the FSR sensors can be used to quantize the irregular gait of an amputee subject, their generalization to the real-world situations are only possible under simplifications.

We show that for a non-trained individual the gait phase within a 1.3 to 1.4 seconds lasting gait cycle comprising seven gait phases can be specified with a probability of 67% for an amputee and 75% for an non-amputee, respectively. We are convinced that, when considering the gait phases sequence, the classification accuracy in the context of some previous gait phases can be increased significantly. Apart from this, our goal is not primarily to detect the regular level gait but the deviations from it. To this, we are interested in locomotion changes and, that is superficial for us, in irregular muscle activities indicating potentially dangerous situations to the amputee. In future work we will extend the experiments to investigate the transitions between the regular level gait, stopping, and some prosthesis slipping situations. Our goal is to develop a low-latency method for a robust detection of non-standard lower-limb situations using EMG signals.


## Acknowledgment

This work was supported by the German Research Foundation under project numbers PL 471/1-3 within the priority program *Organic Computing*.


## References


[1] Perry, J., *Gait Analysis. Normal and Pathological Function*. Slack Int. Book Distributors, 1992.

[2] L. J. Hargrove, H. Huang, A. E. Schulz, B. A. Lock, R. Lipschutz, and T. A. Kuiken, "Toward the Development of a Neural Interface for Lower Limb Prosthesis Control," in *Proceedings 31st Annual International Conference of the IEEE EMBS*. IEEE Computer Society, 2009, pp. 2111–2114.

[3] J. L. Johansson, D. M. Sherrill, P. O. Riley, P. Bonato, and H. Herr, "User-adaptive control of a magnetorheological prosthetic knee," *American Journal of Physical Medicine and Rehabilitation*, vol. 84, no. 8, pp. 563–575, 2005.

[4] M. J. Highsmith, J. T. Kahle, S. L. Carey, D. J. Lura, R. V. Dubey, and W. S. Quillen, "Kinetic Differences Using a Power Knee and C-Leg While Sitting Down and Standing Up: A Case Report," *Journal of Prosthetics Orthotics*, vol. 22, no. 4, pp. 237–243, 2010.

[5] Ossur Bionics, "The Power Knee," http://bionics.ossur.com/pages/306.

[6] R. L. Waters, J. Perry, D. Antonelle, and H. Hislop, "Energy cost of walking of amputees: the influence of level of amputation," *Journal of Bone and Joint Surgery*, vol. 58, no. 1, pp. 42–46, 1976.

[7] D. A. Winter, *The biomechanics and motor control of human gait: normal, elderly and pathological*. Waterloo Biomechanics, 1991.

[8] R. Psonak, "Transfemoral prosthetics," *Orthotics and Prosthetics in Rehabilitation*, 2000.

[9] A. Bar, G. Ishai, P. Meretsky, and Y. Koren, "Adaptive microcomputer control of an artificial knee in level walking," *Journal of Biomedical Engeneering*, vol. 5, no. 2, pp. 145–150, 1983.

[10] B. Hudgins, P. Parker, and R. N. Scott, "A new strategy for multifunction myoelectric control," *IEEE Trans. Biomed. Eng.*, vol. 40, no. 1, pp. 82–94, 1993.

[11] Pappas, I., Popovic, M., Keller, T., Dietz, V., Morari, M., "A Reliable Gait Phase Detection System," in *IEEE Tr. Neural systems and Rehabilitation Engineering*, 2001.

[12] H. Huang, T. A. Kuiken, and R. Lipschutz, "A Strategy for Identifying Locomotion Modes using Surface Electromyography," *IEEE Transactions on Biomedical Engineering*, vol. 56, no. 1, pp. 65–73, 2009.

[13] Liu, T., Inoue, Y., Shibata, K., "Development of a wearable sensor system for quantitative gait analysis," *Measurement*, vol. 42, 2009.

[14] Kong, K., Tomizuja, M., "Smooth and Continuous Human Gait Phase Detection Based on Foot Pressure Patterns," in *2008 IEEE International Conference on Robotics and Automation*, 2008.

[15] Mijailovic, N., Gavrilovic, M., Rafajlovic, S., "Gait Phases Recognition from Accelerations and Ground Reaction Forces: Application of Neural Networks," *Telfor Journal*, vol. 1, 2009.

[16] S. Allen, I. F. Waerlop, and R. Lardner, "The Basics of Gait," *Dynamic Chiropractic*, vol. 25, no. 23, 2007.

[17] National Instruments, `http://sine.ni.com`.

[18] Biovision, `http://www.biovision.eu`.

[19] K. Glette, T. Gruber, P. Kaufmann, J. Torresen, B. Sick, and M. Platzner, "Comparing Evolvable Hardware to Conventional Classifiers for Electromyographic Prosthetic Hand Control," in *Proceedings 3nd NASA/ESA Conference on Adaptive Hardware and Systems (AHS'08)*. IEEE Computer Society, 2008, pp. 32–39.

[20] C. J. C. Burges, "A Tutorial on Support Vector Machines for Pattern Recognition," *Data Mining and Knowledge Discovery*, vol. 2, no. 2, pp. 121–167, 1998.

[21] V. Vapnik, *Statistical Learning Theory (Information Science and Statistics)*. Springer, 2000.